

## **Short report: Imaging-assisted time-resolved dentine sampling to track weaning histories**

Andrea Czermak<sup>1\*</sup>, Lothar Schermelleh<sup>2</sup>, Julia Lee-Thorp<sup>1</sup>

<sup>1</sup> Research Laboratory for Archaeology and the History of Art, School of Archaeology, University of Oxford, UK

<sup>2</sup> Micron Advanced Bioimaging Unit, Department of Biochemistry, University of Oxford, UK

\* Corresponding author. Research Laboratory for Archaeology and the History of Art, School of Archaeology, University of Oxford, 1-2 South Parks Road, Oxford OX1 3TG, United Kingdom. E-mail: andrea.czermak@arch.ox.ac.uk.

Running title: Imaging-assisted time-resolved dentine sampling to track weaning histories

Keywords: Dentine microsampling, chronological age, carbon and nitrogen isotope analysis

Short report: max. 3000 words

Figures: 4

Tables: 1

### **Abstract**

Tooth dentine serial sampling followed by isotope analyses allows detection of shifts in an individual's diet during the periods of tooth formation, providing information on breastfeeding, weaning and childhood nutrition. Current sampling methods, however, do not fully capture the potential resolution of dentine increments because of the difficulties caused by the conical growth pattern, and changes in growth rate during tooth development results in uncertain timing. Here we present an imaging-assisted microsampling approach that takes the biological growth pattern of dentine into account in an effort to improve temporal resolution. We used high-resolution light microscopy images of first molar longitudinal thin sections to generate an accurate optical reference of growth pattern, and formulated a new scheme to assign collected microsamples to age. This allowed us to track dietary changes over more precisely constrained, shorter time periods, providing greater detail and resolution for the

breastfeeding and weaning process. We applied our method to track early life dietary history in four individuals from a small cemetery in Alsace, France, dated to the early 5th century AD (the Late Antique/Migration period). Even within this short time-scale,  $^{13}\text{C}/^{12}\text{C}$  and  $^{15}\text{N}/^{14}\text{N}$  ratio sequences suggest variability in diets, weaning periods and hints of earlier maternal mobility.

## Introduction

The weaning process is a transitional period marked by reduction in the frequency of breastfeeding and increasing consumption of complementary foods. Obtaining a more detailed insight into this transitional period, its length and timing, is of special interest for population studies (for review see Humphrey 2014). During exclusive breast-feeding, an infant obtains all his or her nutrition from mother (or wet nurse), representing approximately one trophic level. This difference is reflected in nitrogen ( $^{15}\text{N}/^{14}\text{N}$ )<sup>1</sup> and sometimes in carbon ( $^{13}\text{C}/^{12}\text{C}$ ) isotope ratios. During weaning breast milk is gradually replaced by protein from complementary ordinary foods that are of a lower trophic level, resulting in a decrease of approximately 2-3 ‰ in  $\delta^{15}\text{N}$ . Earlier approaches relying on isotope ratios in the bone collagen of infants of estimated age of death suffer from problematic age estimation of infants and rapid bone turnover (for review see Reynard & Tuross, 2015).

Thus, dentine sequential sampling has become increasingly popular as an option to obtain a more precise chronology for the diet of an individual from birth to the age of completion of the latest forming tooth. Dentine grows sequentially from the crown to the root tip, forming incremental features with consistent periodic repeat intervals<sup>2</sup>. Teeth do not remodel and the timing of tooth formation is well known (e.g. Dean et al., 1993; AlQahtani et al., 2010). The composition of dentine from incremental structures preserves a record of diet and health conditions during the period of formation that can be related to histologically determined ages (Tang et al., 2016; Dean, 2017). Serial sampling that follows the growth pattern potentially provides a time-resolved isotopic record of dietary intake that can give detailed information about potential changes in nutrition, such as occurs during breastfeeding and weaning.

The standard sampling method is to cut multiple transverse sections from the crown to the root of demineralized teeth, usually the M1, at regular intervals (e.g. Eerkens et al., 2011;

---

<sup>1</sup> By convention, stable isotope ratios are expressed in the  $\delta$  notation, in parts per thousand (per mille or ‰) relative to an international standard, as  $\delta^x\text{Z} = (\text{R}_s/\text{R}_{\text{ref}} - 1) \times 1000$ , where R = isotope ratio ( $^{13}\text{C}/^{12}\text{C}$ ,  $^{15}\text{N}/^{14}\text{N}$ ). The international references for  $^{13}\text{C}/^{12}\text{C}$  and  $^{15}\text{N}/^{14}\text{N}$  are Pee Dee belemnite (PDB) and Ambient Inhalable Reservoir (AIR) respectively.

<sup>2</sup> For detailed description of tooth microstructure see Supporting Information S2.

Beaumont et al., 2013; 2015, Henderson et al., 2014; Sandberg et al. 2014). Transverse sectioning, however, does not adequately consider biological growth pattern. Cutting in this way, through rather than along, increments smears the resulting isotopic sequence considerably and makes assigning samples to chronological age problematic (Makarewicz & Sealy, 2015; Guiry et al., 2016). A dilemma in addressing this problem is that increments are not visible in demineralized teeth. Cutting out ‘point samples’ along the growth axis of the tooth using a biopsy punch (Burt and Garvie-Lok, 2013; Fernandez et al., this volume) or sampling shallow rasters (Guiry et al., 2016) minimizes sampling across multiple incremental layers and thus several growth stages.

Assigning samples to the respective age at which the tooth section formed remains a major difficulty (Henderson, 2014; Humphrey, 2014). Beaumont et al. (2015) presented a diagrammatic timeline for each human tooth approximating the age at formation of respective tooth sections. The ‘*Beaumont-chart*’, however, is designed for horizontally cut, regular-sized dentine sections assuming that each represents the same growth period. But growth layers form at oblique angles to the enamel-dentine and cement-dentine junction (e.g. Dean, 2017)<sup>3</sup>. Further, tooth formation stages are not equally spaced in time, particularly in the crown section (Liversidge, 2015), resulting in potential loss of resolution and uncertainty in timing.

Our goal was to take the directionality of incremental growth structures into account so as to improve the temporal resolution and thus to provide a more accurate representation of alterations in diet within small time-spans. To visualize the dental microstructure, we use microscope images of tooth longitudinal sections and developed a micro-sampling approach that is applicable to demineralized teeth based on data adapted from the *London Atlas of Tooth Development and Eruption* (AlQahtani et al., 2010), which is sensitive to the developmental trajectory. As proof of concept we apply our method to extract small, spatially confined samples to follow small-scale changes in nutrition in four individuals from the Late Antique/Migration Period cemetery of Niedernai in Alsace (France).

## **Material and Methods**

### *Material*

Four first lower molars out of a sample of 17 adults buried at the Late Antique/Migration Period cemetery of Niedernai, Alsace (France) were selected, based on good collagen preservation using fluorescence screening (Czermak et al., forthcoming). The site is dated to the 5th century AD, representing the transformative time during ‘*the great migrations of*

---

<sup>3</sup> For detailed description of tooth development see Supporting Information S2.

people' between Antiquity and Early Middle Ages (see Supporting Information S1).

#### *Assignment of samples to chronological age*

To estimate the approximate chronological age represented by each M1 dentine section, we developed a scheme based on the *London Atlas of Tooth Development and Eruption* (AlQahtani et al., 2010). We used developmental stages recognisable in demineralized teeth (Figure 1) and used the median age as a “*terminus ante quem*”: as dentine has formed to a certain stage by a specific age, any sample from before this stage represents dietary intake by this age.

#### *Sampling<sup>4</sup>*

Mandibular first molars were bisected longitudinally. A ~70 µm thin-section of the mid-part of the tooth was removed and mounted on a microscopy slide (Figure 2, A). Mosaics of transmission light microscopy images were taken<sup>5</sup> to visualize the dentine increments ('Andresen lines') of the entire tooth section (Figure 2 B). One tooth half was demineralized prior sampling (Beaumont et al., 2013). To minimize smearing caused by cutting through incremental layers, we reduced sampling depth by removing the posterior side of the tooth, leaving a ~1.5 mm thick longitudinal dentine section. We applied two complementary sampling methods for refined standard and fine sampling (Figure 2, C): (1) slicing the root from crown to apex into micro-chunks and (2) taking fine slices from the centre of the crown. Sampling was done under a dissecting microscope, using transmission microscope images of the corresponding thin section as optical reference to track the course of the incremental features of each tooth (Figure 2, B).

(1): Micro-chunks: One side of the tooth half, preferentially the mesial root due to its longer root, was cleaned to avoid sampling degraded collagen, the posterior side was removed (see supporting information S3) and then the sampling area was cut into micro-chunks of ≤1 mm width following the natural growth line as closely as possible, using the high-resolution transmission microscopy image as a reference (Figure 2 B). To minimize cutting across incremental layers, the sectioning angle was gradually changed to approximately 45° angles at pulp level (the further downward the root-tip the smaller the angle, at the root-tip cutting almost parallel to the pulp-channel).

(2): Crown thin sections: Samples were collected from the central area of the tooth

---

<sup>4</sup> For detailed description of the sampling procedure see Supporting Information S3.

<sup>5</sup> Mosaic images were taken with a GE DeltaVision DV core wide-field microscope using a 4x/0.16NA air UPlanSApo objective (Olympus) and stitched using GE's softWoRx acquisition software.



crown by slicing the crown into thin parallel sections of ~0.5 mm thickness from the top towards the pulp chamber.

The positions of these samples were assigned according to developmental stages adopted from the *London Atlas of Tooth Development and Eruption* (AlQahtani et al. 2010) (Figure 1 and 3), taking any dental wear into account.

Dentine samples were transferred into micro-tubes without any further treatment and lyophilized ('chunk method' described by Sealy et al. 2014, see Supporting Information S3).

Bone collagen of each individual was extracted to compare diet in early life with adult diet. Samples were weighed into tin capsules and introduced to a SERCON 20/22 continuous flow ratio mass-spectrometer for measurement of carbon and nitrogen isotopes<sup>6</sup>.

## Results

These methods provided 16-20 microsamples from each tooth, of which 4-8 were from the crown section (method 2). Isotopic results assigned to age are shown in Table 1, complete isotopic results and collagen quality criteria are provided in the Supporting Information S5.

For all individuals, cusp tip microsamples show initial high  $\delta^{15}\text{N}$  values. A 'plateau' is visible in the individuals lacking any cusp attrition (16 and 35) (Figure 4). A decline in  $\delta^{15}\text{N}$  values is apparent around the age of 0.5-1 year, levelling off at values about ca. 3-5‰ lower and similar to those of corresponding bone data. Small deviations in the decline trajectory of individuals 16 and 47 are visible in crown section samples (*method 2*). A steeper decent of  $\delta^{15}\text{N}$  in individual 47 suggests a shorter transition-time from exclusive breast-feeding.

Smaller decreases in  $\delta^{13}\text{C}$  are visible (0.5-1‰), but they do match the  $\delta^{15}\text{N}$  patterns, and are thus consistent with the trophic level offset. One exception is the earliest samples of individual 47, which show comparatively high  $\delta^{13}\text{C}$  values of -16‰, gradually declining by ~3‰ to the starting level of the other individuals. This finding strongly suggests an unusual  $\text{C}_4$ -rich diet of the breastfeeding mother. Supplementary and later food was  $\text{C}_3$ -based as for all the other individuals and their bone collagen  $\delta^{13}\text{C}$  values.

## Discussion

The point at which the onset of weaning is isotopically detectable by a decrease in  $\delta^{15}\text{N}$  ratios caused by significant quantities of protein obtained from non-breast milk sources is commonly reported as 'weaning age' (Nitsch et al., 2011; Reynard and Tuross, 2015). The weaning process typically may begin approximately from the age of 6 months when

---

<sup>6</sup> For detailed of collagen extraction methods and isotope analysis see Supporting Information S3.

additional dietary intake from complementary foods is essential to provide all the nutritional requirements of an infant (Kramer & Kakuma, 2012). Initial high  $\delta^{15}\text{N}$  values are visible in all individuals' M1's, while the expected 'plateau' representing a period of exclusive breastfeeding (Humphrey 2014) was only observed in individuals with unworn cusps (individuals 16 and 35). In these individuals, however, the age of weaning onset (as judged by shifts in  $\delta^{15}\text{N}$ ) seems to occur at least 6 months later than the age at which dietary supplementation would become necessary. Possibly supplementary foods may have no significant impact on  $\delta^{15}\text{N}$  ratios by then (Humphrey 2014).

Alternatively, the corresponding tooth may have developed slightly earlier than assigned. We used the median age of completion for developmental stages from the *London Atlas*, but there are variations in the timing of the growth of the dentition between individuals (AlQahtani et al., 2010) thus leading to potential timing differences when comparing dietary values of the same developmental stage between individuals. On the other hand, there is little variation in the age at which the crown stages are completed. Hence, while tooth formation stages are not equally spaced in time (Liversidge, 2015), samples taken in between two stages *should* cover a similar timespan. The *London Atlas* is currently the most accurate dental age estimation method, but precisely assigning microsample samples to age in *individuals* remains problematic.

Due to the increased temporal resolution, we could detect a short-term increase in the otherwise gradually decreasing  $\delta^{15}\text{N}$  trajectories in the crown sections of individuals 16 and 47, indicating a diet temporarily richer in protein, perhaps a short-term return to breastfeeding. Furthermore, the  $^{13}\text{C}$ -enriched composition in individual 47 indicates a  $\text{C}_4$  isotope signal<sup>7</sup>, suggesting a significant proportion of millet in the individuals' mothers diet passed on through her breast-milk. Millet was relatively uncommon in the Early to Middle Ages in Central and Western Europe, therefore its appearance raises the possibility of female mobility. The crown section of M1 is clearly the tooth developmental region of interest for breastfeeding and weaning. While 'conventional' sampling would have provided at most 5 samples for this time span, micro-sampling the crown centre provides additional 4-8 samples, thus representing a considerable resolution improvement in sampling surviving adults.

The presented imaging-assisted microsampling approach was aimed to take the directionality of incremental growth structures into account as advocated by Humphrey (2014) and Guiry (2016), so as to improve the temporal resolution and thus to provide a more accurate

---

<sup>7</sup> Marine fish consumption can be excluded due to the location of the cemetery and the archaeological context (cf. Supporting Information S1).

representation of alterations in diet within small time-spans. By collecting micro-samples from tooth dentine, especially from the crown area, we obtained a finer temporal resolution of dietary intake during the weaning process. Correlated transmission microscopy of dentine microstructure allows to identify incremental lines and thus to sample alongside the direction of dentine growth. We are also able to assign subsamples taken from the crown area (2) to samples taken from the root (1) (Figure 2D and 3). While long-period lines are relatively easy to detect in the crown section, they become less visible in the root area even in higher-resolution images. Dentine tubules, however, are readily visible in light microscopy and run roughly transverse to the increments. Thus, the course of the tubules may be used as indicator for the growth-direction of the increments. We recommend cutting approximately at a right angle to the visible tubules or alternatively, if no microscope is available, adjusting the cutting angle as described in sampling method 1 above.

It is important to note that dentine and the collagen structure need to be intact, as only well-preserved dentine keeps its firm structure after tooth demineralisation. This is key for the sectioning method that requires no breakages and gaps. It is particularly important for the high-resolution crown sections to provide enough material for the fine slices. The high density of sampling points, especially in the crown section representing the weaning period, provides relatively smooth, yet for each individual, slightly different trajectories that are coherent and lack outliers.

We suggest that the time-resolved microsampling approach described here provides a more precise means to reconstruct profiles of dietary changes during the first years of an adult individual's life.

**Conflict of interest:** The authors declare no conflict of interest.

**Author contributions:** A.C. conceived the project and performed experiments. L.S. contributed with microscopy and image processing. J.L-T. provided facility and advice for isotope analysis and microsampling. A.C. wrote the manuscript with input of all authors.

**Acknowledgements**

We are grateful to Peter Ditchfield (University of Oxford) for technical support with mass spectrometry, and Professor Tim Watson (Dental Institute, Kings College London) for advice on dental morphology and sampling strategies. This research was funded by the Deutsche Forschungsgemeinschaft (DFG) and the Agence Nationale de la Recherche (ANR) as part of the NiedArch's collaborative research project (principal investigators: Susanne Brather-Walter and Eckhard Wirbelauer). We would like to thank Eric Guiry and an anonymous reviewer who helped to significantly improve this manuscript.

### **Supplementary information**

Supplementary data related to this article can be found in the online edition. These include:

S1 Material

S2 Tooth development

S3 Detailed description of Methods

S4 Supplementary references

S5 Supplementary table

### **References**

AlQahtani SJ, Hector MP, Liversidge HM. 2010. Brief communication: the London Atlas of human tooth development and eruption. *American Journal of Physical Anthropology* 142: 481-490.

Beaumont J, Gledhill A, Lee-Thorp JA, Montgomery J. 2013. Childhood diet: a closer examination of the evidence from dental tissues using stable isotope analysis of incremental human dentine. *Archaeometry* 55: 277-295.

Beaumont J, Gledhill A, Lee-Thorp JA, Montgomery J. 2015. Oral histories: a simple method for assigning chronological age to isotopic values from human dentine collagen. *Annals of Human Biology* 42 (2): 407-414.

Burt NM, Garvie-Lok S. 2013. A new method of dentine microsampling of deciduous teeth for stable isotope ratio analysis. *Journal of Archaeological Science* 40: 3854-3864.

Czermak, A. Schermelleh, L., Lee-Thorp, J., forthcoming. Fluorescence screening of collagen preservation in tooth dentine.

Dean C, Beynon AD, Reid DJ, Whittaker DK. 1993. A longitudinal study of tooth growth in a single individual based on long- and short- period incremental markings in dentine and enamel. *International Journal of Osteoarchaeology* 3: 249-264.

Dean C. 2017. How the microstructure of dentine can contribute to reconstructing developing dentitions and the lives of hominoids and hominins. *Comptes Rendus Palevol* 16 (5-6): 557-571. <http://dx.doi.org/10.1016/j.crpv.2016.10.006>.

Eerkens JW, Berget AG, Bartelink EJ. 2011. Estimating weaning and early childhood diet from serial micro-samples of dentin collagen. *Journal of Archaeological Science* 38: 3101-3111.

Fernández-Crespo T, Czermak A, Lee-Thorp JA, Schulting RJ. (this volume). Being a child in Late Neolithic north-central Iberia. Breastfeeding, weaning and childhood diet in Alto de la Huesera megalithic grave through sequential dentine and bone collagen stable isotope analyses.

Guiry EJ, Hepburn JC, Richards MP. 2016). High-resolution serial sampling for nitrogen stable isotope analysis of archaeological mammal teeth. *Journal of Archaeological Science* 69: 21-28.

Henderson RC, Lee-Thorp J, Loe L. 2014. Early life histories of the London poor using  $\delta^{13}\text{C}$  and  $\delta^{15}\text{N}$  stable isotope incremental dentine sampling. *American Journal of Physical Anthropology* 154: 585-593.

Humphrey LT. 2014. Isotopic and trace element evidence of dietary transitions in early life. *Annals of Human Biology* 41 (4): 348-357.

Kramer MS, Kakuma R. 2012. Optimal duration of exclusive breast-feeding. *Cochrane Database System Rev* 8: CD003517. DOI: 10.1002/14651858.CD003517.pub2.

Liversidge HM. 2015. Controversies in age estimation from developing teeth. *Annals of Human Biology* 42 (4): 397-406.

Makarewicz C, Sealy JC. 2015. Dietary reconstruction, mobility, and the analysis of ancient skeletal tissues: Expanding the prospects of stable isotope research in archaeology. *Journal of Archaeological Science* 56: 146-158.

Nitsch E, Humphrey LT, Hedges REM. 2011. Using stable isotope analysis to examine the effect of economic change on breastfeeding practices in Spitalfields, London, UK. *American Journal of Physical Anthropology* 146: 619–628.

Reynard LM, Tuross N. 2015. The known, the unknown and the unknowable: weaning times from archaeological bones using nitrogen isotope ratios. *Journal of Archaeological Science* 53: 618-625.

Sandberg PA, Sponheimer M, Lee-Thorp JA, van Gerven D. 2014. Intra-tooth stable isotope analysis of dentine: a step toward addressing selective mortality in the reconstruction of life history in the archaeological record. *American Journal of Physical Anthropology* 55: 281-293. DOI: 10.1002/ajpa.22600

Sealy JC, Johnson M, Richards MP, Nehlich O. 2014. Comparison of two methods of extracting bone collagen for stable carbon and nitrogen isotope analysis: comparing whole bone demineralization with gelatinization and ultrafiltration. *Journal of Archaeological Science* 47: 64-69.

Tang N, Le Cabec A, Antoine D. 2016. Dentine and cementum structure and properties. in: *A Companion to Dental Anthropology*, Chapter 15. edit. Joel D. Irish, G. Richard Scott. John Wiley & Sons, Inc.: 202-222.







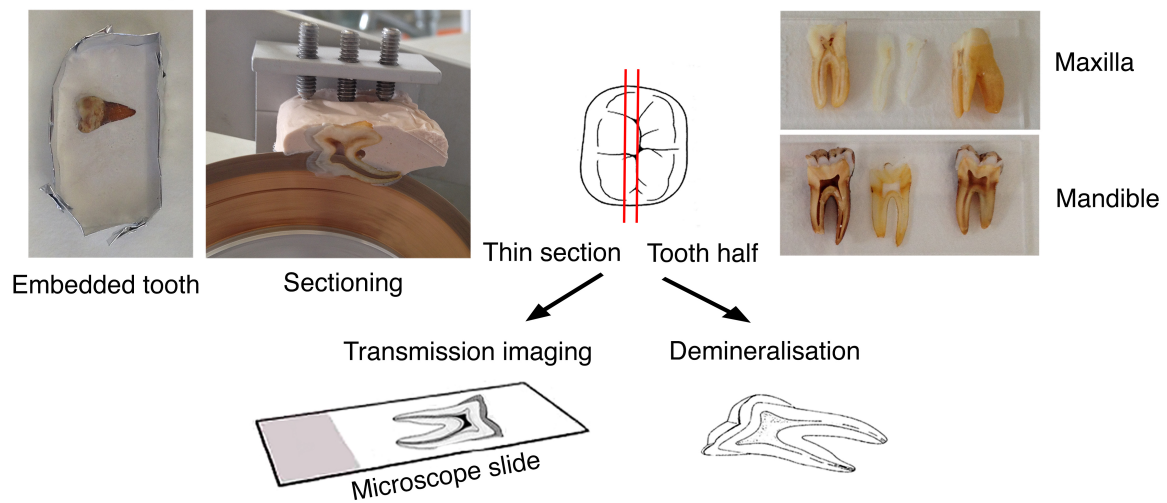
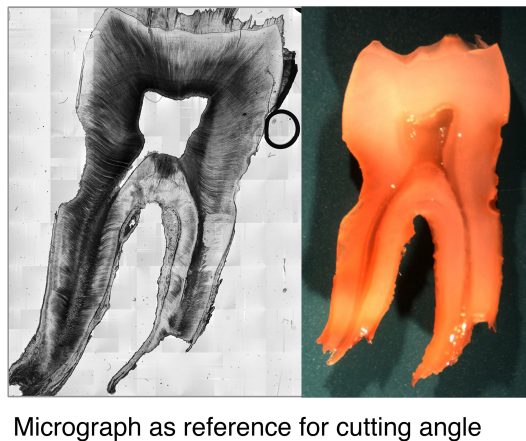
Mandible					M1
Developmental stages					
Microsampling		London Atlas:		Completed by:	
I	Initial cusp formation	Ci		Early – Late	Birth – 4.5 m
				Median	0.25y
C	Cusp outline complete	Coc		Early – Late	7.5m – 1.5y
				Median	1.5 y
P	Pulp roof	Crc		Early – Late	2.5 –4.0
				Median	3.0
F	Furcation	R 1/4		Early – Late	4.0 – 6.5
				Median	5.0
R 1/2	Half root	R 1/2		Early – Late	4.5 – 7.0
				Median	6.5
R	Root completed	Rc		Early – Late	7.0 – 10.5
				Median	8.5

Figure 1: Developmental stages of M1 comprehensible in demineralized dentine: **(I)** Initial cusp formation, **(C)** Cusp outline complete, **(P)** Pulp roof defined, **(F)** Root bifurcation, **(R)** Root length complete. The stage of the half completed root (**R 1/2**) can roughly be estimated. Median, minimum and maximum age of completion of each stage is presented for the first molar. Stages and data are adopted from the *London Atlas of Tooth Development and Eruption* (AlQahtani et al., 2010).

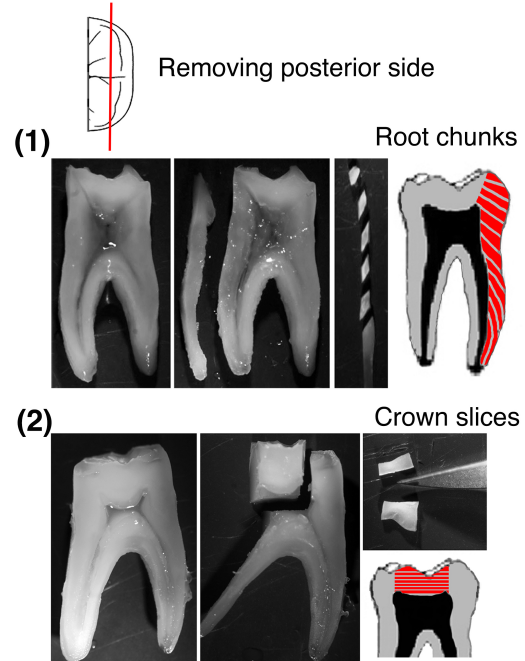
## A Sectioning



## B Microscopy and imaging



## C Dentine sampling



## D Matching incremental features

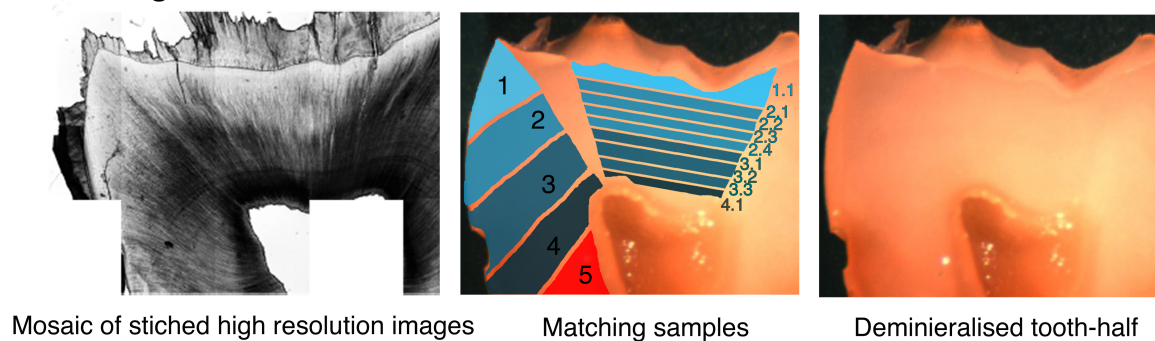


Figure 2: Dentine serial-sampling workflow. A: Sectioning. Bisecting the tooth longitudinally and taking a  $\sim 70\mu\text{m}$  thin section. B: Microscopy and imaging. ‘Mosaic’ of consecutive series of transmission light microscopy images and stitched to a high-resolution image of the entire tooth section. Processing the image in ImageJ/Fiji. C:



Dentine sampling. Removing the posterior side of the tooth-half. (1) Cutting chunks along the root. (2) Taking micro-slices from crown centre. D: Matching incremental features. Samples taken from the crown centre (2) are matched with the corresponding samples taken from the root (1) using high-resolution images.

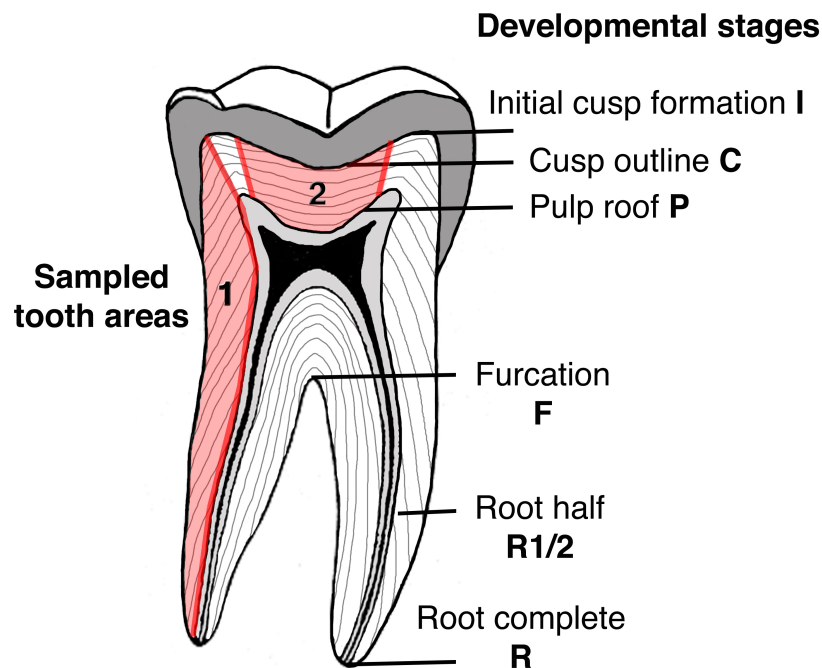


Figure 3: Tooth developmental stages used as reference to assign micro-samples to age according to the 'London Atlas of Tooth development and Eruption' (AlQahtani et al., 2010), and sampled tooth areas.

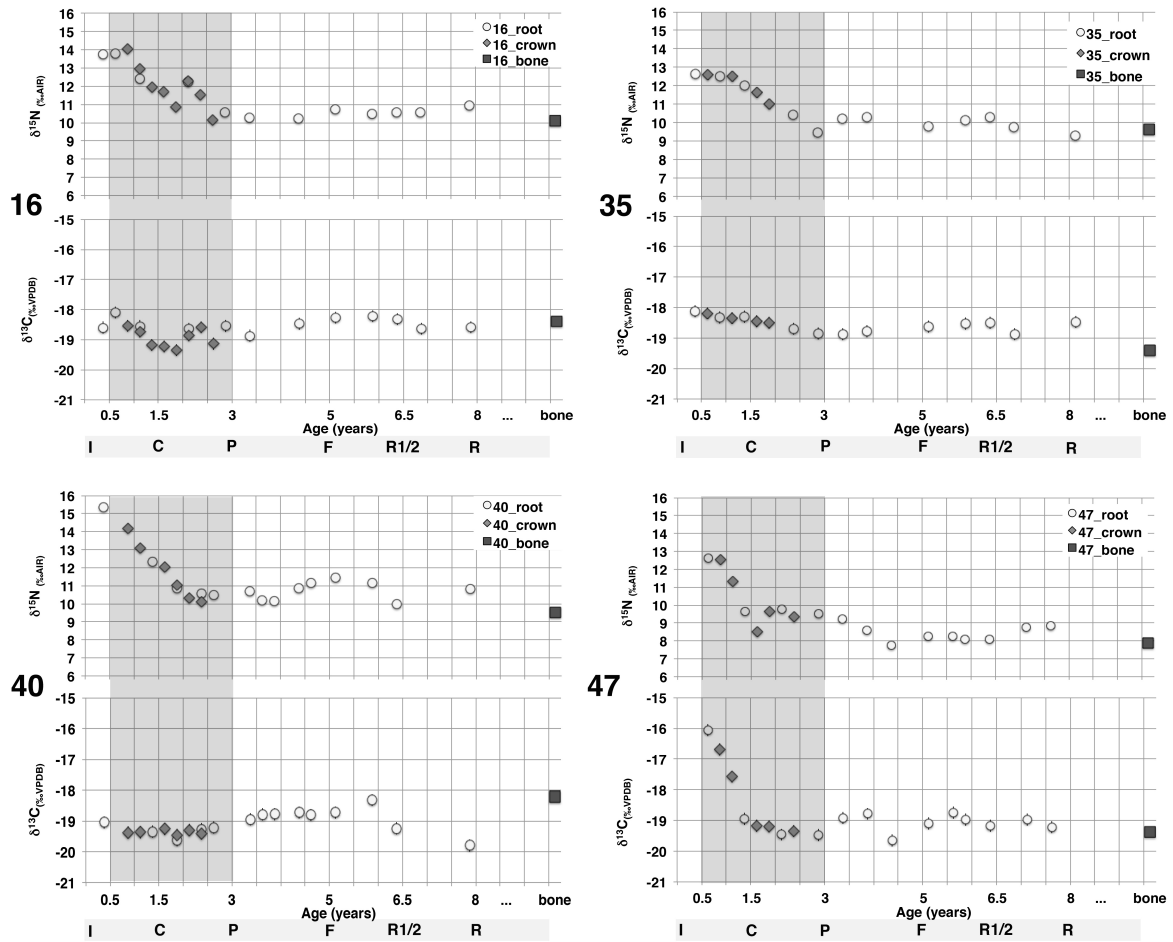


Figure 4: Time-resolved isotope analysis results of tooth dentine micro-samples. Dark symbols: samples from the crown centre. Light symbols: samples taken from complete tooth length. Initials of tooth developmental stages see Figure 1 and 3. Approximate time period covered by higher-resolution samples from the crown area shaded in grey.

Individual		16		35		40		47	
Stages	Age	$\delta^{15}\text{N}_{(\text{AIR})}$ )	$\delta^{13}\text{C}_{(\text{VPDB})}$	$\delta^{15}\text{N}_{(\text{AIR})}$	$\delta^{13}\text{C}_{(\text{VPDB})}$	$\delta^{15}\text{N}_{(\text{AIR})}$	$\delta^{13}\text{C}_{(\text{VPDB})}$	$\delta^{15}\text{N}_{(\text{AIR})}$	$\delta^{13}\text{C}_{(\text{VPDB})}$
I	0								
	0.5	13.76	-18.60	12.63	-18.12	15.37	-19.05		
C	1.5	13.78	-18.10	C 12.59	C -18.19	C 14.20	-19.38	12.62	-16.06
		C 14.05	C -18.54	12.51	-18.33			C 12.52	C -16.69
		C 12.95	C -18.73	C 12.50	C -18.34	C 13.08	-19.37	C 11.34	C -17.58
		12.43	-18.55						
		C 12.25	C -19.17	12.02	-18.31	12.32	-19.35	9.94	-18.95
P	3	C 12.27	C -19.23	C 11.63	C -18.45	C 12.04	C -19.26	C 8.52	C -19.17
		C 11.96	C -19.34			C 11.04	C -19.63	C 9.64	C -19.19
		11.69	-18.64	C 11.01	C -18.50	10.85	-19.47	9.77	-19.46
		C 11.53	C -18.85			C 10.58	C -19.30		
		10.86	-18.59	10.41	-18.69	10.50	-19.40	C 9.33	C -19.34
		C 10.16	C -19.14			C 10.31	C -19.27		
F	5	10.57	-18.55	9.46	-18.85	C 10.12	C -19.22		
								9.52	-19.47
		10.27	-18.87	10.22	-18.87	10.68	-18.95	9.22	-18.91
						10.18	-18.79		
				10.30	-18.79	10.14	-18.79	8.59	-18.78
		10.22	-18.47			10.85	-18.92	7.76	-19.66
R 1/2	6.5					11.14	-18.81		
		10.75	-18.26	9.78	-18.62			8.26	-19.11
						11.45	-18.73		
		10.49	-18.63	10.15	-18.53			8.49	-18.75
						11.16	-18.32	8.08	-18.97
		10.58	-18.09	10.30	-18.50				
R	8					9.97	-19.25	8.10	-19.18
		10.55	-18.58	9.75	-18.87			8.75	-18.98
								8.83	-19.21
		10.96	-18.29			10.84	-19.80		
...	Bone			9.28	-18.47				
		10.11	-18.39	9.61	-19.40	9.54	-18.22	7.88	-19.37

Table 1: Isotope analysis results of dentine samples of four individuals buried on the Niedernai cemetery assigned to age/developmental stages of the tooth. Micro-samples were taken from the root and from the crown centre of the tooth.

## Supplementary Information

### Imaging-assisted time-resolved dentine sampling to track weaning histories

Andrea Czermak<sup>1\*</sup>, Lothar Schermelleh<sup>2</sup>, Julia Lee-Thorp<sup>1</sup>

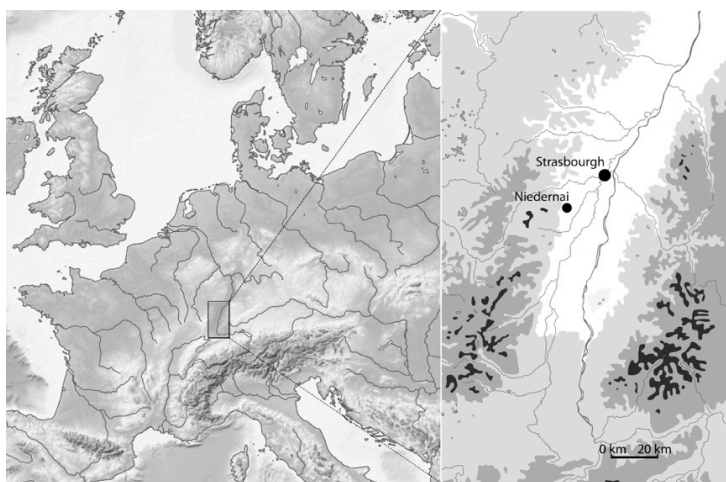
<sup>1</sup> Research Laboratory for Archaeology and the History of Art, School of Archaeology, University of Oxford, UK

<sup>2</sup> Micron Advanced Bioimaging Unit, Department of Biochemistry, University of Oxford, UK

#### S.1 Material

The small burial site of Niedernai is located in the upper Rhine valley (Alsace, France), at the (former) Roman Rhine frontier (Figure S1). The cemetery was in use for a relatively short period, representing about two generations and dates from the mid 5th to the early 6th century AD. Individuals lived in the transformative period during ‘the great migrations of people’ between Antiquity and the Early Middle Ages. As a region at the border of the “barbarian world” during Roman times, the upper Rhine valley became centre stage in a newly established cultural and political zone ruled by Frankish monarchs in the mid-sixth century (e.g. Hen 2007). The collapse of the Roman social order is believed to have had profound effects on the population’s culture, identity, and daily life.

Of a total of 21 burials, teeth of 18 individuals were available for dentine serial sampling. First permanent molars of four individuals out of the sample of 17 adults were selected, based on fluorescence screening (Czermak et al., forthcoming). However, following demineralisation, dentine structure was found to be sound enough, across the entire section in four individuals reported here, to carry out sampling method 2 (micro-slicing the crown area). Rib samples were taken for each individual.



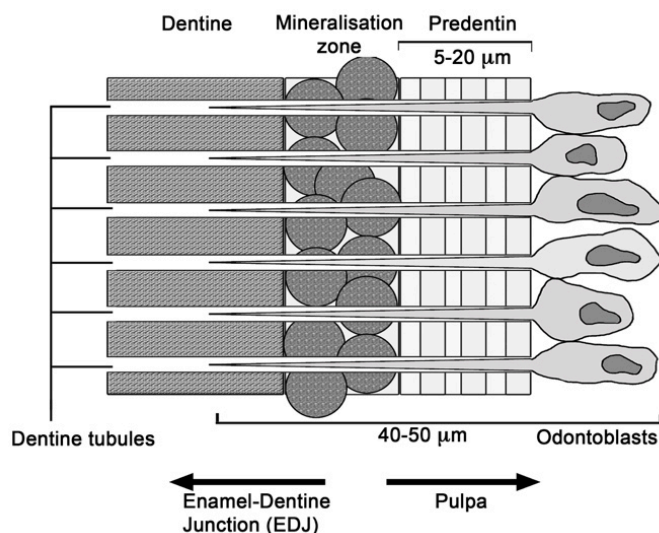
Supplementary Figure S1: Location of Site. The burial site of Niedernai is located in the upper Rhine valley (Alsace, France).

## S.2 Tooth development and microstructure

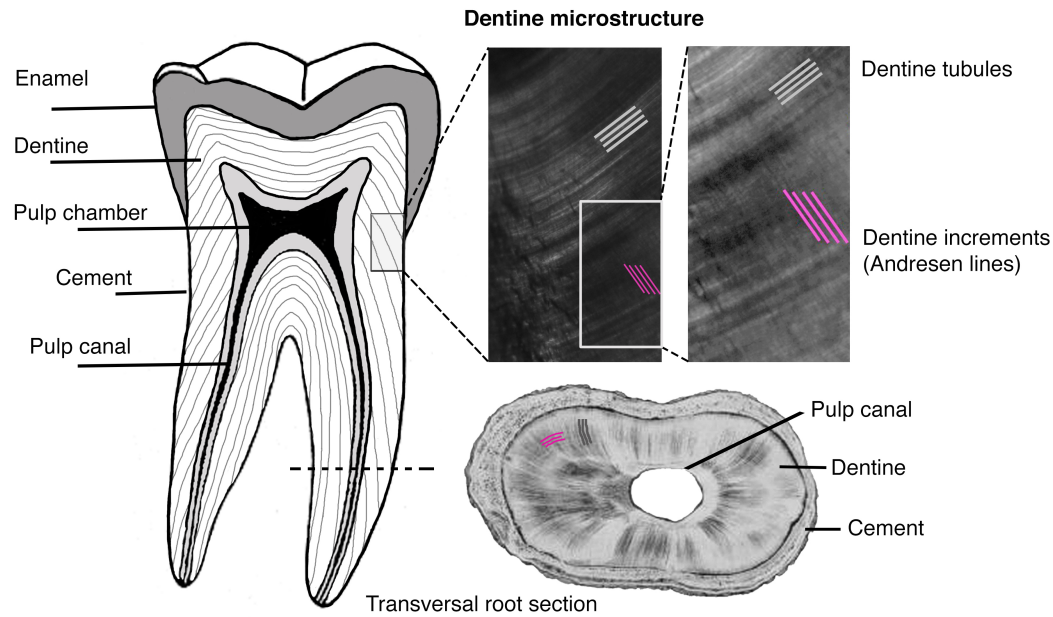
The timing of the development of human teeth, and the direction and rate of growth and mineralisation is well established (Beniash 2011; Dean 2017). Dentine formation initiates at the enamel/dentine junction (EDJ) of the crown. Periods of active secretion and mineralization alternate with resting periods. Resting phases, in which the mineralization stops, appear as contours in micrographs (Schroeder 2000). Incremental features include both long- and short-period increments, ranging from (sub)-daily to annual periodicity.

Odontoblasts, accommodated in the dentine tubules, secrete pre-dentine, which is then mineralized along its collagen fibers with bioapatite crystals secreted from odontoblast extensions. The retreating odontoblasts move away from the enamel/dentine junction (EDJ) towards the pulp chamber, producing dentine layer by layer (Figure S2). Root dentine grows from the cement/dentine junction (CDJ) (see Schroeder, 2000; Beniash, 2011). Growth layers form at oblique angles to the EDJ and CDJ (e.g. Dean et al., 1993). The daily secretion rate of dentin in human teeth ranges from 2 to 6  $\mu\text{m}/\text{day}$ , resulting in short-period lines ('von Ebner's lines'). Long period lines ('Andresen lines') are formed every 8-10 days with a width ranging from 20-30  $\mu\text{m}$  (e.g. Kawasaki 1980; Dean 1995, 1998, 2017; Schroeder, 2000; Smith 2006, 2008). Here we focus on the long-term dentine incremental structures known as Andresen lines. In transmission light micrographs Andresen lines reveal as contrasting linear patterns, transverse to the direction of the dentinal tubules (Figure S3). For review on dentine microstructure see Dean (2017).

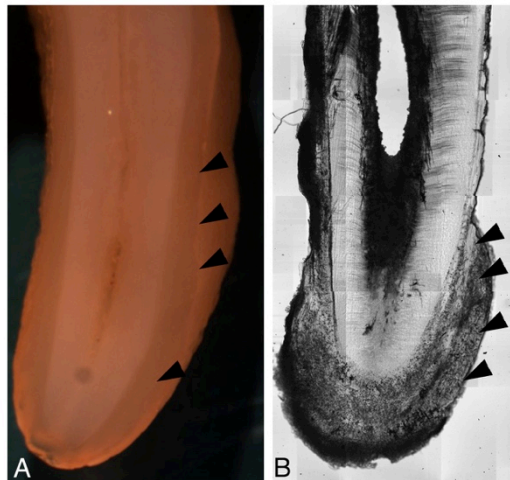
After the tooth is fully developed and the formation of primary dentine is complete, other dental tissues continue to form throughout life (Schroeder 2000): (1) secondary dentine is continually developed in small layers by the odontoblasts on the wall of the pulp chamber. (2) Tooth cement, growing from the middle third of the root to the apex in circa-annual layers and becomes thicker in older individuals (e.g. Wittwer-Backofen 2004). We removed these secondary features (see Figure S4).



Supplementary Figure S2: Schematic diagram of dentine formation (figure modified after Schroeder 2000).



Supplementary Figure S3: Tooth structure and dentine microstructure. High-resolution images of dentine showing dentinal tubules (grey) and dentine increments ('Andresen lines') (magenta).



Supplementary Figure S4: Dental cement. (A) Demineralized tooth half. Thick cementum layer is visible on the exterior side of the root (arrows). (B) Micrograph of a thin section of the same tooth. Cementum partially chipped off during the cutting process.

## **S.3 Methods**

### **S.3.1 Dentine**

#### **Sectioning**

Tooth samples were cleaned mechanically with water to remove debris from the surface. Teeth were embedded in Herculite II (a high-strength gypsum molding material), leaving the mesial or distal root surface exposed so as to be able to target where exactly to bisect the tooth longitudinally. The teeth were then bisected using a Buehler Isomet low-speed diamond saw with a micrometer gauge, abrasive wafering blade and a cooling water bath.

Further, a  $\sim 70\mu\text{m}$  thin section was made. In mandibular teeth, the more precise cut tooth-half was chosen for dentine sampling; in maxillary teeth the buccal part of the root was used, saving the lingual root part (see Figure 2, main manuscript). The lingual bisection was saved for future analysis. Tooth enamel was carefully removed using a hand-held drill, leaving the EDJ intact, and saved for further analysis.

#### **Microscopy and image processing**

The longitudinal thin-section from the center part of the tooth was mounted on a microscopy slide using Eukitt quick hardening mounting medium (Sigma Aldrich). A consecutive series of transmission light microscopy images were taken in a raster ('mosaic') on a GE DeltaVision DV core wide-field microscope using a 4x/0.16NA air UPlanSApo objective (Olympus). These were then stitched to a high-resolution image of the entire tooth section using GE's softWoRx acquisition software to visualize the dentine increments of this section. Images were then processed in ImageJ/Fiji (Schindelin, 2012). First a linear contrast correction was applied (all images same scaling): 12-bit image (0-4096 grey scale levels), followed by a Gamma correction (Filter 0.5-0.7) to enhance the contrast of poorly visible dark areas without saturating the brighter areas.

#### **Serial microsampling and collagen extraction**

We customized our sampling strategy by combining established sampling and extraction methods. Dentin was prepared for sampling using the *Beaumont method 2*, i.e., sectioning after demineralization (Beaumont et al., 2013). For collagen extraction we combined two methods (see Sealy et al., 2014; Jørkov et al. 2007). First, we applied a modified *Chunk method* (Sealy et al. 2014), i.e., demineralizing and freeze-drying chunks, skipping gelatinization and ultra-filtration. However, we omitted the NaOH-step, as described in the *Extraction method C* by Jørkov et al. (2007), which is effectively the approach described by Richards and Hedges (1999), but leaving out ultrafiltration steps.

Although NaOH and ultra-filtration steps are frequently employed at this point to eliminate possible contaminants such as humic acids, we avoided these steps to minimize collagen loss in the small samples. We also ensured that humic contamination was minimal based on visual inspection (colour). This was further monitored by C/N ratios (below).



### *Demineralisation*

Tooth halves were demineralized in 0.5 M hydrochloric acid (HCl) solution in glass vials at 4°C. The acid was changed every other day until the teeth appeared translucent and flexible, indicating complete decalcification. Demineralization process took from three to about ten days, presumably depending on the individual density of the tooth mineral. In well-preserved teeth, demineralization yields a collagen 'pseudomorph' (Sealy et al., 2014), keeping the same shape and almost the same size as the original tooth. Poorly preserved teeth become more amorphous or may completely dissolve in HCl. Samples were rinsed three times and soaked in deionized water for three days, changing the water every day until pH was neutral.

### *Microsampling*

We applied two sampling methods: (1) slicing the root from crown to apex into micro-chunks and (2) taking fine slices from the centre of the crown. Sequential microsampling of the demineralized tooth half was done under a dissecting stereo-microscope (Olympus SZX) (alternatively, an optical loupe can be used). Transmission microscope images of the corresponding thin section were used as optical reference to track the course of the incremental features of each tooth. The tooth was cut on a Harris cutting mat with a scalpel, undertaken as follows:

#### (1): Chunk method:

- Any visible dental-cement was removed by scraping the cementum off the root surface with a scalpel (see Figure S4).
- The sampling area was then separated from the tooth body by cutting longitudinally alongside the pulp canal and then, reaching the pulp chamber, in an angle towards the crown tip (Fig. 3). Any material from the inner root furcation area was discharged to avoid secondary dentine.
- As dentin growth layers form at oblique angles rather than linear to the enamel-dentine junction and bend concentrically around the pulp, the sampling area was sectioned longitudinally and the posterior side was removed to minimize cutting through incremental layers by reducing sampling depth (see Guiry et al., 2016), leaving a remaining ~1.5 mm thick longitudinal slice.
- To minimize contamination from deposits in the exposed root canal, soft material was removed from the pulp-canal and pulp-chamber by gently scraping the surface with a scalpel.
- The remaining ~1.0-1.5 mm wide longitudinal tooth slice was sampled sequentially from the crown to the apical root using a scalpel. The dentine was cut into micro-chunks of  $\leq 1$  mm width following the natural growth line as closely as possible, using the individual high-resolution transmission microscopy image (obtained prior to demineralisation) as a reference. To minimize cutting across incremental layers, the sectioning angle was gradually changed to approximately 45° angles at pulp level (the further downward the root-tip the smaller the angle, at the root-tip cutting almost parallel to the pulp-channel). (see Figure 2, main manuscript).

An average of 12 samples per tooth was possible with this sampling strategy (see Figure 4, main manuscript).

## (2): Crown thin sections

- The central area of the tooth crown (Fig. 3, area 2) was separated from the remaining tooth.
- Again, the posterior side was removed to minimize cutting through incremental layers by reducing sampling depth (Guiry et al. 2016), leaving a ~1.0-1.5 mm thick dentine piece.
- Samples were collected by slicing the crown into thin parallel sections of ca. 0.5 mm thickness from the crown towards the pulp chamber. The layer immediately adjacent to the pulp chamber was discarded to minimize contamination (see method 1).

The positions of all samples were recorded and assigned according to developmental stages adopted from the *London Atlas of tooth development and Eruption* (AlQahtani et al. 2010) (Figs. 1 and 3), taking any dental wear into account. Both methods combined provided 16-20 microsamples from each tooth, of which 4-8 were from the crown section. High-resolution images were used to match the samples taken from the crown centre with the corresponding sample taken from the root (see Figure 4D, main document).

Dentine samples were transferred into micro-tubes and a hole was punched in the lid of each tube with a pin to allow the liquid to evaporate, after which the samples were lyophilized for 4-6 h.

After freeze-drying the small solid dentine sticks or thin slices were weighed and transferred into tin capsules. Typical sample sizes were between 0.5 and 0.8 mg. Since low mass samples produce insufficient CO<sub>2</sub> and N<sub>2</sub> for precise isotopic measurement (e.g. Burt and Amin, 2014), samples <0.4 mg were merged with either the previous or next sample, depending on position according to the developmental stages (Fig. 3). Subsamples taken from the crown area were too big (>1.4g) in some cases. In this case the thin slices were shortened, taking the growth direction of the increments into account.

Dentine samples were transferred into tin capsules and sorted by mass into three groups: (1) 0.4-0.5 mg, (2) 0.6-0.8 mg, (3) 0.9-1.3 mg. Weights of the standard analysed alongside the unknowns were adjusted accordingly. Standards were interspersed throughout each analytical run, about 60% samples, 40% standards.

### S.3.2 Bone

The fragments of ribs were cleaned mechanically in water to remove soil from the surface, ultrasonicated in purified water and then allowed to dry for ~4 days. The dry samples were finely ground in a mortar and pestle. Collagen was extracted according to *extraction method C* (see Jørkov et al., 2007), which is a modified method by Richards and Hedges (1999), omitting ultra-filtration. Samples were demineralized in 0.5 M HCl at 4°C for ~1 week and then gelatinized at 75°C for 48 hours in pH 3 dH<sub>2</sub>O. NaOH pre-treatment was not carried out. The demineralized sections were rinsed with deionized water and placed in sealed microtubes with a pH 3 HCl solution at 70°C for 48 h to denature the collagen. Debris at the base of the microtubes was removed after centrifugation. No filtration was carried out. The samples were first frozen and then freeze-dried. About 1.0 mg of the extracted bone collagen was then weighed into tin capsules.

### S.3.3 Isotope analysis

Samples were loaded into a SERCON 20/22 continuous flow isotope ratio mass spectrometer coupled with an elemental analyzer for measurement of carbon and nitrogen isotopes. By convention, stable isotope ratios are expressed in the  $\delta$  notation, in parts per thousand (per mil or ‰) relative to an international standard, as

$\delta^xZ = (R_s/R_{ref} - 1) \times 1000$ , where  $R$  = isotope ratio ( $^{13}\text{C}/^{12}\text{C}$ ,  $^{15}\text{N}/^{14}\text{N}$ ) and the international standards for  $^{13}\text{C}/^{12}\text{C}$  and  $^{15}\text{N}/^{14}\text{N}$  are Vienna Pee Dee Belemnite (VPDB) and Ambient Inhalable Reservoir (AIR) respectively.

Analytical precision for both isotopes is  $\pm 0.2\text{‰}$  ( $1\sigma$ ) based on repeated analyses of internal (alanine, marine seal collagen, bovine collagen) and international standards (caffeine IAEA 600).

Bone samples were measured in duplicate. Dentine microsamples were not measured in duplicate, firstly because of the small yield and secondly because the unique samples represent a particular timespan and it is impossible to precisely replicate the sample elsewhere e.g. on the opposite root. However, the dual sampling approach using both the crown dentine that overlaps partly with the root serves as an internal control, as root-chunk sample measurements should yield an average of the isotope values from the corresponding crown-subsamples (see Figure 2, main manuscript).

Collagen integrity was assessed according to standard criteria, including %C and %N and C/N ratios (Ambrose, 1990; DeNiro, 1985; van Klinken, 1999). A conservative C/N ratio of 2.9-3.4 was used (rather than 2.9-3.6 used by De Niro, 1985; van Klinken, 1999) given the small sample size and the lack of duplicate dentine measurements. In intact collagen %C values should be  $34.8 \pm 8.8$  wt%, and %N values 11-16 wt% (van Klinken, 1999, Oxford  $^{14}\text{C}$  database). Higher values of the former can be an indicator for contamination with non-protein contaminants (Ambrose, 1990).

#### S.4 Supplementary references

AlQahtani SJ, Hector MP, Liversidge HM. 2010. Brief communication: The London atlas of human tooth development and eruption. *American Journal of Physical Anthropology* 142(3): 481-90.

Ambrose SH. 1990. Preparation and characterization of bone and tooth collagen for isotopic analysis. *Journal of Archaeological Science* 17(4): 431-451.

Beaumont J, Gledhill A, Lee-Thorp J, Montgomery J. 2013. Childhood diet: a closer examination of the evidence from dental tissues using stable isotope analysis of incremental human dentine. *Archaeometry* 55(2): 277-295.

Beniash E. 2011. Biominerals – hierarchical nanocomposites: the example of bone. *Nanomedicine and Nanobiotechnology* 3 (1): 47-69.

Burt N.M., Amin M. 2014. A mini me? Exploring early childhood diet with stable isotope ratio analysis using primary teeth dentin. *Archives of Oral Biology* 59 (11): 1226-1232.

Coplen, T. B. 2011, Guidelines and recommended terms for expression of stable-isotope-ratio and gas-ratio measurement results, *Rapid Communications in Mass Spectrometry*, 25 (17), 2538-60.

Czermak, A. Schermelleh, L., Lee-Thorp. J., forthcoming. Fluorescence screening of collagen preservation in tooth dentine.

Dean M.C., Beynon A.D., Reid D.J., Whittaker D.K. 1993. A longitudinal study of tooth growth in a single individual based on long- and short-period incremental markings in dentine and enamel. *International Journal of Osteoarchaeology* 3: 249-264.

Dean M.C., Saundrett A.E. 1995. Rates of Dentine Mineralization in Permanent Human Teeth. *International Journal of Osteoarchaeology* 5: 349-358.

Dean M.C. 1998. Comparative observations on the spacing of short-period (von Ebner's) lines in dentine. *Archives of Oral Biology* 43 (12): 1009-1021.

Dean C. 2017. How the microstructure of dentine can contribute to reconstructing developing dentitions and the lives of hominoids and hominins. *Comptes Rendus Palevol* 16 (5-6): 557-571. <http://dx.doi.org/10.1016/j.crpv.2016.10.006>.

DeNiro M.J. 1985. Post-mortem preservation and alteration of in vivo bone collagen isotope ratios in relation to palaeodietary reconstruction. *Nature* 317: 806-809.

Guiry E.J., Hepburn J.C., Richards M.P. 2016. High-resolution serial sampling for nitrogen stable isotope analysis of archaeological mammal teeth. *Journal of Archaeological Science* 69: 21-28.

Jørkov M.S., Heinemeier J., Lynnerup N. 2007. Evaluating bone collagen extraction methods for stable isotope analysis in dietary studies. *Journal of Archaeological Science* 34: 1824-1829.

Kawasaki K., Tanaka S., Ishikawa T. 1980. On the daily incremental lines in human dentine. *Archives of Oral Biology* 24: 939-943.

Richards, M.P., Hedges, R.E.M., 1999. Stable isotope evidence for similarities in the types of marine foods used by Late Mesolithic humans at sites along the Atlantic coast of Europe. *Journal of Archaeological Science* 26, 717-722.

Sandberg PA, Sponheimer M, Lee-Thorp JA, van Gerven D. 2014. Intra-tooth stable isotope analysis of dentine: a step toward addressing selective mortality in the reconstruction of life history in the archaeological record. *American Journal of Physical Anthropology* 55: 281-293. DOI: 10.1002/ajpa.22600

Schindelin, J.; Arganda-Carreras, I., Frise, E. et al. (2012), "Fiji: an open-source platform for biological-image analysis", *Nature Methods* 9: 676-682.

Schroeder H.E. 2000. Orale Strukturbilogie / Oral Structural Biology (German version). Thieme Verlag Stuttgart.

Sealy J, Johnson M, Richards MP, Nehlich O. 2014. Comparison of two methods of extracting bone collagen for stable carbon and nitrogen isotope analysis: comparing whole bone demineralization with gelatinization and ultrafiltration. *Journal of Archaeological Science* 47: 64-69.

Smith T. 2006. Experimental determination of the periodicity of incremental features in enamel. *Journal of Anatomy* 208, 99-113.

Smith T. 2008. Incremental dental development: Methods and applications in hominoid evolutionary studies. *Journal of Human Evolution* 54 (2), 205-224.

van Klinken GJ. 1999. Bone collagen quality indicators for palaeodietary and radiocarbon measurements. *Journal of Archaeological Science* 26 (6): 687-695.

Wittwer-Backofen U., Gampe J., Vaupel J.W. 2004. Tooth Cementum Annulation for age estimation: results from a large known-age validation study. *American Journal of Physical Anthropology* 123: 119-129.

## S.5 Supplementary table

Dentine and bone collagen isotope data. According to %C and %N quality criteria the data are in the upper range of the tolerated scale, which may be due to NaOH-purification step was left out and the collagen was not gelatinised to avoid collagen loss. However, a more conservative C:N ratio of 2.9-3.4 was used. (Data labelled in grey were excluded).

Sample	Weight (g)	%N (wt%)	%C (wt%)	C/N (molar)	$\delta^{15}\text{N}_{(\text{AIR})}$ (‰)	$\delta^{13}\text{C}_{(\text{VPDB})}$ (‰)
16_root_1	1.0	15.0	41.9	3.2	13.8	-18.6
16_root_2	1.6	16.9	46.1	3.2	13.8	-18.1
16_root_3	1.3	15.1	42.0	3.2	12.4	-18.6
16_root_4	1.1	15.2	41.8	3.2	12.3	-18.6
16_root_5	0.9	20.7	42.5	2.4	10.0	-18.9
16_root_6	1.4	15.3	42.3	3.2	10.6	-18.5
16_root_7	1.0	15.3	42.4	3.2	10.3	-18.9
16_root_8	1.2	15.5	43.0	3.2	10.2	-18.5
16_root_9	1.4	15.4	42.6	3.2	10.8	-18.3
16_root_10	1.4	15.3	42.4	3.2	10.5	-18.2
16_root_11	1.5	15.4	42.4	3.2	10.6	-18.3
16_root_12	1.1	15.3	42.6	3.2	10.6	-18.6
16_root_13	1.3	15.3	42.4	3.2	11.0	-18.6
16_crown_1	1.0	15.2	42.3	3.3	14.1	-18.5
16_crown_2	1.3	15.2	42.4	3.2	13.0	-18.7
16_crown_3	0.7	14.9	42.4	3.3	12.0	-19.2
16_crown_4	0.8	15.1	43.0	3.3	11.7	-19.2
16_crown_5	0.5	14.9	42.4	3.3	10.9	-19.3
16_crown_6	1.2	15.1	42.3	3.3	12.3	-18.9
16_crown_7	1.4	17.0	47.5	3.3	11.5	-18.6
16_crown_8	1.1	14.9	42.5	3.3	10.2	-19.1
16_bone	1.5	15.1	42.1	3.3	10.1	-18.4
35_root_1	0.4	15.6	43.8	3.3	12.6	-18.1
35_root_2	0.5	15.1	41.3	3.2	12.5	-18.3
35_root_3	1.0	16.1	43.0	3.1	12.0	-18.3
35_root_4	0.7	15.9	43.0	3.2	10.4	-18.7
35_root_5	0.7	16.1	43.6	3.2	9.5	-18.8
35_root_6	0.7	15.9	43.1	3.2	10.2	-18.9
35_root_7	0.8	16.0	43.2	3.2	10.3	-18.8
35_root_8	0.8	16.0	43.1	3.2	9.8	-18.6
35_root_9	0.9	16.0	43.1	3.1	10.1	-18.5
35_root_10	0.7	16.6	45.0	3.2	10.3	-18.5
35_root_11	0.7	15.2	41.0	3.2	9.7	-18.9
35_root_12	0.5	15.7	42.9	3.2	9.3	-18.5
35_crown_1	0.6	15.4	43.0	3.3	12.6	-18.2
35_crown_2	0.5	15.4	43.4	3.3	12.5	-18.3
35_crown_3	0.4	15.5	43.2	3.3	11.6	-18.4
35_crown_4	0.7	15.6	42.6	3.2	11.0	-18.5
35_bone	1.1	15.1	41.7	3.2	9.6	-19.4

Sample	Weight (g)	%N (wt%)	%C (wt%)	C/N (molar)	$\delta^{15}\text{N}_{(\text{AIR})}$ (‰)	$\delta^{13}\text{C}_{(\text{VPDB})}$ (‰)
40_root_1	0.8	15.9	43.2	3.2	15.4	-19.1
40_root_2	0.4	15.9	44.2	3.2	12.3	-19.4
40_root_3	0.6	15.3	42.6	3.2	10.9	-19.6
40_root_4	0.8	15.5	42.2	3.2	10.6	-19.3
40_root_5	0.8	15.6	42.8	3.2	10.5	-19.2
40_root_6	0.8	15.7	42.9	3.2	10.7	-18.9
40_root_7	0.6	15.8	43.4	3.2	10.2	-18.8
40_root_8	0.6	15.8	43.6	3.2	10.1	-18.8
40_root_9	0.7	16.1	44.0	3.2	10.8	-18.7
40_root_10	0.7	16.1	44.2	3.2	11.1	-18.8
40_root_11	0.7	16.0	43.8	3.2	11.4	-18.7
40_root_12	0.5	15.8	43.8	3.2	11.2	-18.3
40_root_13	0.8	15.9	43.3	3.2	10.0	-19.2
40_root_14	0.6	15.8	43.3	3.2	10.8	-19.8
40_crown_1	0.8	15.9	43.3	3.2	14.2	-19.4
40_crown_2	0.8	15.3	41.8	3.2	13.1	-19.4
40_crown_3	0.6	15.9	43.6	3.2	12.0	-19.3
40_crown_4	0.6	15.8	43.2	3.2	11.0	-19.5
40_crown_5	0.6	16.0	44.0	3.2	10.3	-19.3
40_crown_6	0.8	15.9	43.3	3.2	10.1	-19.4
40_bone	1.1	15.7	42.8	3.2	9.5	-18.2
47_root_1	1.0	15.5	42.2	3.2	12.6	-16.1
47_root_2	0.4	15.5	42.0	3.2	9.6	-18.9
47_root_3	0.9	15.6	42.5	3.2	9.8	-19.5
47_root_4	0.8	15.3	42.0	3.2	9.5	-19.5
47_root_5	0.9	15.6	42.7	3.2	9.2	-18.9
47_root_6	0.5	15.5	42.2	3.2	8.6	-18.8
47_root_7	0.4	15.7	42.8	3.2	7.8	-19.7
47_root_8	0.9	15.6	42.4	3.2	8.3	-19.1
47_root_9	0.6	15.4	42.2	3.2	8.3	-18.8
47_root_10	0.7	15.4	42.6	3.2	8.1	-19.2
47_root_11	0.6	15.5	43.0	3.2	8.8	-19.0
47_root_12	1.0	15.3	41.8	3.2	8.8	-19.2
47_crown_1	0.8	15.5	42.3	3.2	12.5	-16.7
47_crown_2	0.7	15.6	41.8	3.1	11.3	-17.6
47_crown_3	0.6	15.6	42.6	3.2	8.5	-19.2
47_crown_4	1.0	15.4	41.8	3.2	9.6	-19.2
47_crown_5	0.8	16.9	46.2	3.2	9.3	-19.3
47_bone	1.0	16.7	45.8	3.2	7.9	-19.4